RESEARCH ARTICLE

Maloperation of Zone-3 Distance Relay Prevention Using Distribution Entropy

UPENDRAN MUKUNDARAJAN[ID] AND K. SHANTI SWARUP[ID], (Senior Member, IEEE)

Department of Electrical Engineering, Indian Institute of Technology Madras, Chennai 600036, India

Corresponding author: Upendran Mukundarajan (upendranramanujam@gmail.com)

ABSTRACT Maloperation of third-zone distance relays is predominantly caused by power swings, load encroachment, and voltage instability events. Another possibility for third-zone distance relay maloperation is a delayed voltage recovery event. If the impedance trajectory enters the zone-3 reach of a distance relay owing to a delayed voltage recovery event, it can be identified using the severity index-based method. However, the same method requires a relay margin index to be calculated, which is possible only if the impedance trajectory lies outside the zone-3 reach following fault clearance. If the impedance trajectory lies inside the zone-3 reach, even after the fault clearance and event changes from a fault to a delayed voltage recovery event, then there is a chance of maloperation of the third zone distance relay. The proposed method using distribution entropy identifies fault occurrence and fault clearance events critically which is been used in the distance relays for IEEE 39 bus test system and the results are found to be satisfactory in terms of prevention of maloperation of third zone distance relay during non-fault events and operation during fault events. In addition, the security index of the distance relays with proposed algorithm is enhanced by 20% compared to their operation without algorithm while the dependability index remains same.

INDEX TERMS Delayed voltage recovery, distance relay, distribution entropy, fault clearance, maloperation, zone-3.

I. INTRODUCTION

Distance relays are predominantly used in transmission lines to protect power systems from faults. A distance relay can be used for zone-1, zone-2 and zone-3 protection. A zone-1 distance relay protects 85% of the transmission line from faults, whereas a zone-2 distance relay serves as the primary protection of the line and partially backs up the adjacent lines. If the primary protection fails to operate during a fault, the backup protection must operate and protect the transmission line. A zone-3 distance relay serves as backup protection for the entire length of the adjacent lines [1].

However, third-zone distance relays, which are supposed to operate only for short-circuit faults, maloperate during other power system phenomena such as power swings, load encroachment, and voltage instability events [2]. Maloperation may occur if the impedance trajectory at a zone-3

The associate editor coordinating the review of this manuscript and approving it for publication was Nga Nguyen[ID].

distance relay enters the zone-3 reach during a power swing, load encroachment, or voltage instability event.

In [3], a method based on the time required for the impedance trajectory to cross concentric characteristics was developed. If the time taken for the impedance trajectory to cross the concentric characteristics violates a threshold, it is considered a non fault condition. However, this method cannot identify faults after the relay has been blocked because of non-fault conditions, such as power swing.

In [4], the authors developed a method based on the transient monitoring function and phase angle of the positive-sequence impedance to prevent distance relay maloperation during power swings, load encroachment, and voltage stressed conditions. This method allows distance relays to operate for faults, even during voltage-stressed conditions, if the phase angle of the positive sequence impedance is greater than a preset threshold. However, this method fails to identify a resistance fault since the phase angle of the positive sequence impedance is less than the threshold.

In [5], a method has been developed to identify a stable power swing. A fictitious reactance is determined and the relative speed of the machine is calculated to identify zero crossings, representing stable power swings. However, the method does not consider changes in the network configuration and cannot be applied for online evaluation.

A method based on a two-dimensional decision plane was developed in [6] to block maloperating zone-3 distance relays. The superimposed components of the voltage magnitude are considered as indices to differentiate between fault and non-faulty conditions. If one of the indices is above a preset threshold, and the differences between the indices are above the same threshold, it is identified as a fault. This study mainly focused on discriminating stressed conditions from fault events for different power system disturbances. Additional works for identifying faults during system stressed conditions have been discussed in [7] and [8].

Synchrophasor-assisted protection for the satisfactory operation of distance relays during normal and system stressed conditions was considered in [9], [10], and [11]. The problem of distance relay maloperation due to power swing, load encroachments has been extensively discussed in the literature. However, the maloperation of distance relay due to delayed voltage recovery event is discussed minimally only in [12]. Another work for identifying delayed voltage recovery events proposed in [13] requires real time post fault voltage trajectories for assessment. Considering communication failures and extensive implementation costs, local voltage- and current- based methods are preferred [14].

In [12], the authors developed a blocking index that identifies whether the trajectory is closing onto the third zone of critical distance relays and blocks them from operation during a delayed voltage recovery event. The method determines critical time and critical voltage level at which the trajectory arrives in the third zone of the critical relays using the relay margin index and time variant severity indices. The relay margin index and time variant severity indices are computed based on the assumption that the impedance trajectory, for a zone-3 distance relay, will lie outside the zone-3 characteristic. However, following fault clearance, there can be a case of delayed voltage recovery to 80% of the pre-contingency voltage within 20 seconds, leading to the case of impedance trajectory being inside zone-3 reach. In this scenario, the severity indices based method proposed in [12] cannot be computed and therefore cannot be used.

If the impedance trajectory enters the zone-3 characteristic of a distance relay during a fault and stays inside the zone-3 even after the fault is cleared, for a considerable duration, then there is a chance of maloperation of zone-3 distance relay. Hence, there is a requirement of identifying fault occurrence and clearance events with respect to zone-3 distance relay maloperation. The maloperation of zone-3 distance relay even after the fault clearance has not been reported in the literature.

In [15], an algorithm has been proposed to avoid zone-3 maloperation by identifying the fault occurrence and clearance events using high frequency components. However, there is a requirement of a high sampling frequency of 200 kHz. In [16], the authors have used the approximate entropy method and fast wavelet transform to identify fault occurrence during power swings. The method was used to operate distance relays for faults during power swings. However, a method for blocking distance relay maloperation is not discussed. Moreover, distribution entropy is a computationally efficient method [17] as compared to approximate entropy. Hence, that is used for identifying fault occurrence and clearance in the proposed work.

In the present work, distribution entropy is used for identifying fault occurrence and clearance from the local measurements at a zone-3 distance relay. The distribution entropy of the sending end voltage of the transmission line and the bus at which a zone-3 distance relay is connected, changing beyond a threshold can indicate fault occurrence and clearance. If the impedance trajectory remains inside zone-3 characteristic, for a longer duration, despite fault being cleared, identified through the proposed distribution entropy method, then the relay will be blocked to avoid maloperation.

Section II provides a basic demonstration of the zone-3 distance relay maloperation with a simple test system. Section III explains the proposed distribution entropy method for blocking maloperating relays. The proposed method is implemented on IEEE 39 bus system and the simulation results are presented in Section IV for various case studies. Section V presents the conclusion and future scope of this work. The main contributions of the work are:

- Proposed distribution entropy based method for identifying fault occurrence and clearance events. This does not require high sampling frequency as in [15]. Computationally more efficient than the approximate entropy method and half the reduction in computational time.
- An algorithm has been proposed based on the distribution entropy method to block maloperating distance relays.
- The proposed method works for delayed voltage recovery events where voltage recovers to 80% of pre-contingency voltage within 20 seconds. Severity index based method in [12] not applicable for these cases. Efficiency of the proposed method is demonstrated through extensive simulations.

II. MALOPERATION OF ZONE-3 DISTANCE RELAY

To explain the phenomenon of zone-3 distance relay maloperation, a 9 bus system, as shown in Fig.1 with data given in [18] is considered. Generators are represented as transient two-axis models. An IEEE Type-1 model from [19] is considered for the exciters of the generators connected at buses 2 and 3. Loads at Bus-6 and Bus-8 are considered as in [18]. An induction machine load of 143 MVA, 0.875 pf is considered at Bus-5. The induction machine parameters are
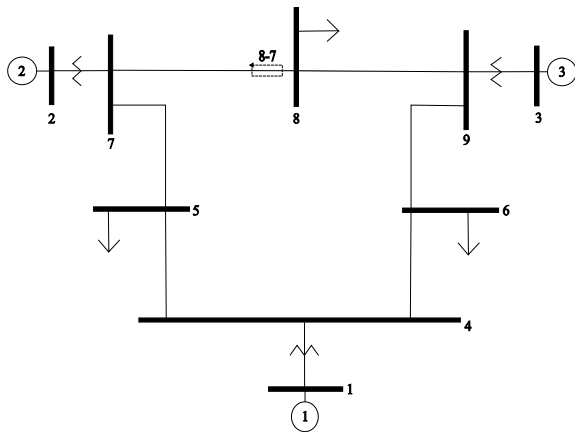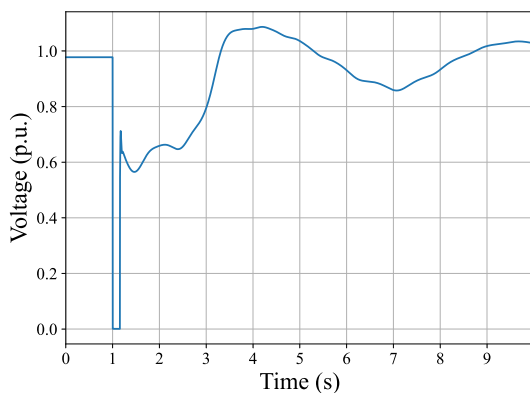
FIGURE 1. 9 bus system.
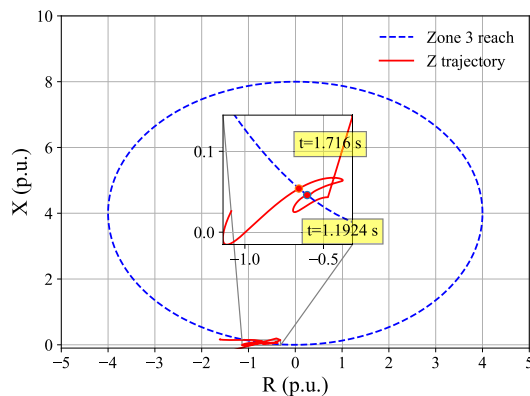

FIGURE 2. Bus 5 Voltage magnitude.

FIGURE 3. DR placed in line between Bus 8-7.

given in [20]. Distance relays (DR) are assumed to be of mho type with characteristic angle equal to line impedance angle.

A three phase bolted fault is applied at Bus-5 at t=1 s, for 150 ms. Bus-5 voltage magnitude with respect to time is given in Fig.2. It can be observed from Fig.2 that after the fault is cleared, there is a delayed voltage recovery and voltage reaches 80% of its prefault value after 2s. The R-X plot of the distance relay, for the line between Bus-8 and Bus-7, that acts as zone-3 protection for the Bus-5 fault is given in Fig.3.

In Fig.3, the characteristics of zone-3 relay are given in blue. It can be observed from the Fig.2 and Fig.3 that even after the fault is cleared at 1.15 s, the R-X trajectory enters the zone-3 characteristic. If the trajectory stays within the characteristics of zone-3 for a period beyond threshold, the relay in line between Bus-8 and Bus-7 will treat it as a fault, even though the fault is cleared. This leads to maloperation of zone-3 relay.

In [12], an algorithm was proposed to block the maloperating zone-3 distance relay. A Time varying Severity Index for voltage ($SI_V(t)$) is proposed as a ratio of the difference between the bus voltage with respect to the nominal voltage each instant of time. The distance between the impedance seen by the distance relay to the supposed intersection point of impedance trajectory on zone-3 characteristic is considered as relay margin (RM) [21]. If $SI_V(t)$ and RM of the distance relay crosses a threshold, the algorithm is activated. The algorithm predicts the possibility of R-X trajectory breaching the zone-3 characteristic and blocks the relay from operation. This method works accurately for the cases where the R-X trajectory is outside and approaching the zone-3 characteristic. However, there is a possibility that R-X trajectory may enter zone-3 characteristic during fault and stays inside the zone-3 reach even after fault clearance during delayed voltage recovery events [22].

There are different cases of voltage recovery trajectories following fault clearance as provided in [22] and [23]. There are cases such as normal recovery 1 as shown in Fig.4, normal recovery 2 and then there is delayed recovery as displayed in Fig.5. In the normal recovery 1 shown in Fig.4, the voltage recovers above 80% of initial voltage following fault clearance, whereas in the delayed recovery case, the voltage can recover back to 80% of the voltage within 20 seconds as depicted in Fig.5. There might be adequate standards and utilities requirements to reduce this time. However, during the time period of voltage sag following fault clearance, if the load pattern is such that (comprises induction machine loads) the impedance trajectory lies inside the zone 3 reach even after the fault clearance, there is a chance of maloperation of zone 3 distance relay. The method in the existing literature considers only the normal recovery 1 whereas with the delayed voltage recovery case, the relay margin and all of the indices could not be calculated if the trajectory lies inside the zone 3 reach. Hence the distance relay may maloperate misinterpreting it to be a fault and therefore fault occurrence and fault clearance event identification is necessary.

Whether the R-X trajectory entering zone-3 is due to a fault or delayed voltage recovery can be assessed by accurately identifying fault occurrence and clearance events. In case, if its identified that fault has occurred and cleared, from the local measurements of zone-3 distance relay, then even if R-X trajectory is present inside zone-3 it can be ascertained that it is due to delayed voltage recovery phenomenon and not because of fault and therefore the relay maloperation should be blocked.
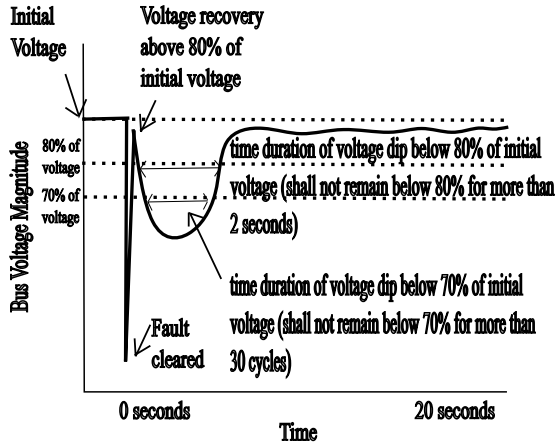
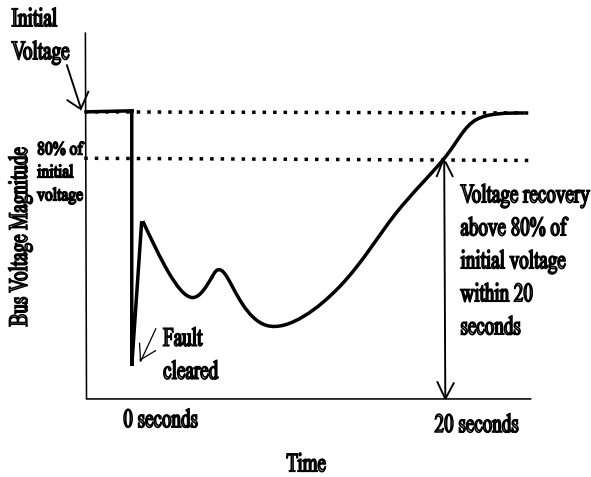**FIGURE 4.** Normal recovery case 1.

FIGURE 5. Delayed recovery.

In [16], the authors have used the approximate entropy method and fast wavelet transform to identify fault occurrence during power swings. However, approximate entropy is computationally not efficient as compared to distribution entropy. The number of operations can be reduced by as high as 50% with distribution entropy. In the present work, a distribution entropy [24] based fault occurrence and fault clearance identification is proposed to prevent the maloperation of zone-3 distance relay and block it. The proposed method will also work for the cases where R-X trajectory enters zone-3 during fault and stays inside even after the fault clearance event, unlike the severity index based method proposed in [12].

III. MALOPERATION OF ZONE-3 DISTANCE RELAY PREVENTION USING DISTRIBUTION ENTROPY BASED ALGORITHM

As mentioned in section II, maloperation of zone-3 distance relay prevention is done using proposed distribution entropy based algorithm.

A. DISTRIBUTION ENTROPY AND MOVING WINDOW VERSION

The steps to calculate distribution entropy from [24] is explained below:

A signal $x[i]$ is sampled at sampling frequency f_{samp} with fundamental frequency of the system being $f_{fundamental}$. This leads to $f_{samp}/f_{fundamental}$ samples per cycle. A moving window of N samples is taken, that is equal to samples of 2-3 cycles is considered.

Considering embedding dimension as m and time delay as τ. For a signal $x[i] : 1 \leq i \leq N$ of length N samples

1) Form $(N - (m - 1)\tau)$ template vectors each of length m

$$X_i^m = x[i + k\tau] : 0 \leq k \leq m - 1$$

2) The maximum distance between individual template vectors are calculated using (1)

$$d_{ij}^m = \max|X_i^m - X_j^m| : 1 \leq j \leq N - (m - 1)\tau, j \neq i \tag{1}$$

3) A distance matrix D of dimension $(N - (m - 1)\tau) \times (N - (m - 1)\tau - 1)$ is formed in (2) and distances are calculated according to (1). The main diagonal elements of the matrix D will be zero and not considered. The matrix will be symmetrical since the mutual distances between individual vectors will be the same. The upper diagonal matrix elements alone are considered in D' as shown in (3).

$$D = \begin{bmatrix} d_{12}^m \cdots & d_{1[N-(m-1)\tau]}^m \\ d_{21}^m \cdots & d_{2[N-(m-1)\tau]}^m \\ .. & \ddots & \vdots \\ .. & .. & d_{[N-(m-1)\tau][N-(m-1)\tau-1]} \end{bmatrix} \tag{2}$$

$$D' = \begin{bmatrix} d_{12}^m & d_{13}^m \cdots & d_{1[N-(m-1)\tau]}^m \\ & d_{23}^m \cdots & d_{2[N-(m-1)\tau]}^m \\ & \ddots & \vdots \\ & & d_{[N-(m-1)\tau][N-(m-1)\tau-1]} \end{bmatrix} \tag{3}$$

4) The distance matrix D' elements are placed in corresponding bins and a histogram is obtained
5) The probability of each bin k is calculated by

$$p_k = \frac{\text{counts in bin k}}{\text{number of elements in the matrix } D'} : 1 \leq k \leq B \tag{4}$$

where B is the number of bins

6) The normalized distribution entropy (H) is obtained by the following relation.

$$H(m, \tau, B) = \frac{-1}{log_2 B} \sum_{k=1}^{B} p_k log_2 p_k \tag{5}$$

Distribution entropy value is a dimensionless quantity as it depends on the logarithm (to the base 2) of the ratio of the
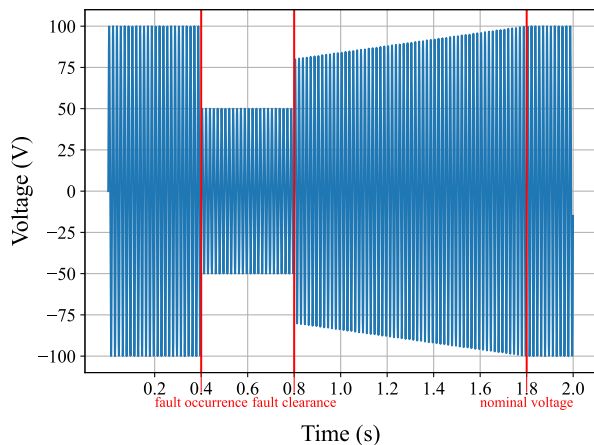
FIGURE 6. Signal.

FIGURE 7. Distribution entropy for fault occurrence and fault clearance event.

count of number of entries in a bin to the total number of entries.

Instead of taking fixed bin numbers, it is better to consider a proper binning method in histogram. According to [25], Freedman Diaconis rule is preferred for binning. f_{samp} is considered as 2.5kHz for a 60 Hz system. Embedding dimension (m) is considered as 2 and time delay (τ) is considered as unity [26]. Moving window length (N) is considered as data length of 100 samples.

The Entropy-Hub application from [27] is used to calculate the distribution entropy for a signal. The steps for obtaining a moving window of distribution entropy is considered the same as that considered for approximate entropy in [28]. The distribution entropy of the instantaneous voltage signal is calculated for every moving window length and assigned to the final sample.

Instead of computing the distribution entropy (H) value at each and every instant, a moving step (α_s) of 10 samples is considered such that the moving window is shifted by that size in the original sequence of the data. The intermediate values of distribution entropy between two moving windows are assigned the previous distribution entropy value.

A test signal as shown in Fig.6 is considered for calculation of distribution entropy. Fault event is considered to be occurring at 0.4 seconds and cleared at 0.8 seconds and voltage recovering back to nominal voltage takes about 1 second. All the events are shown in Fig.6 with red vertical line. Voltage is recovering gradually after fault clearance and attains nominal value at 1.8 seconds. The distribution entropy for the fault occurrence and clearance event for the signal obtained in moving window fashion is shown in Fig.7. The distribution entropy value decreases momentarily during the events and settles back to the initial value.

B. PROPOSED ALGORITHM

The rate of change of voltage magnitude ($\frac{dV_{mag}}{dt}$) is also obtained at every instant. Distribution entropy value of the current data sequence and past two data sequences at α_s and
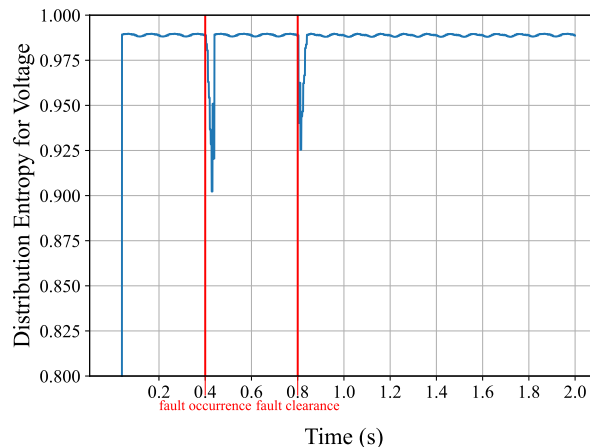
$2\alpha_s$ samples before the present instant x are represented as H[x], H[x-α_s] and H[x-$2\alpha_s$] respectively. The distribution entropy value of the signal during steady state is considered as H_{init}. Th_1, Th_2 and Th_3 are thresholds. H_{flt} and H_{cl} are just represented as the distribution entropy value obtained during fault occurrence and clearance events respectively. The *flag* is initially set as zero.

As represented in Fig.8, the procedure of identifying the maloperating distance relay is checked for all distance relays in the system. All the functions represented are corresponding to any distance relay q.

The proposed algorithm identifies if a fault has occurred using the fault occurrence detection part and makes the *flag* non zero. By means of the drop in the distribution entropy value, and the drop in the voltage magnitude, it is identified as fault occurrence event. If *flag* is set to non zero, then the fault clearance part of the algorithm is made active and fault clearance is identified by drop in distribution entropy value, and sudden increase in the voltage magnitude simultaneously. If fault clearance is detected, then *flag* is set back to zero. Even if the impedance Z seen by the distance relay q lies inside its zone-3 reach, only if *flag* is non zero for a duration of zone-3 time delay τ_{z3d}, then the distance relay q is given the trip command or else the distance relay is blocked from operation.

C. THRESHOLD SELECTION

Thresholds has been selected by choosing the significant drop in the distribution entropy value for worst case scenarios of bolted three phase fault at remote end of adjacent lines and must be greater than worst case generator outage and line outage cases as shown for case studies 4 and 5 in Section IV. Threshold values are obtained by conducting extensive simulations for different contingency scenarios and are fixed. Thresholds Th_1 is considered to be 0.05, Th_2 is considered to be 0.1 *p.u.* $\times f_{samp}$ and Th_3 is considered to be 0.4 for the test system. It is found that the obtained threshold values are satisfactory and operates fine for the test system.
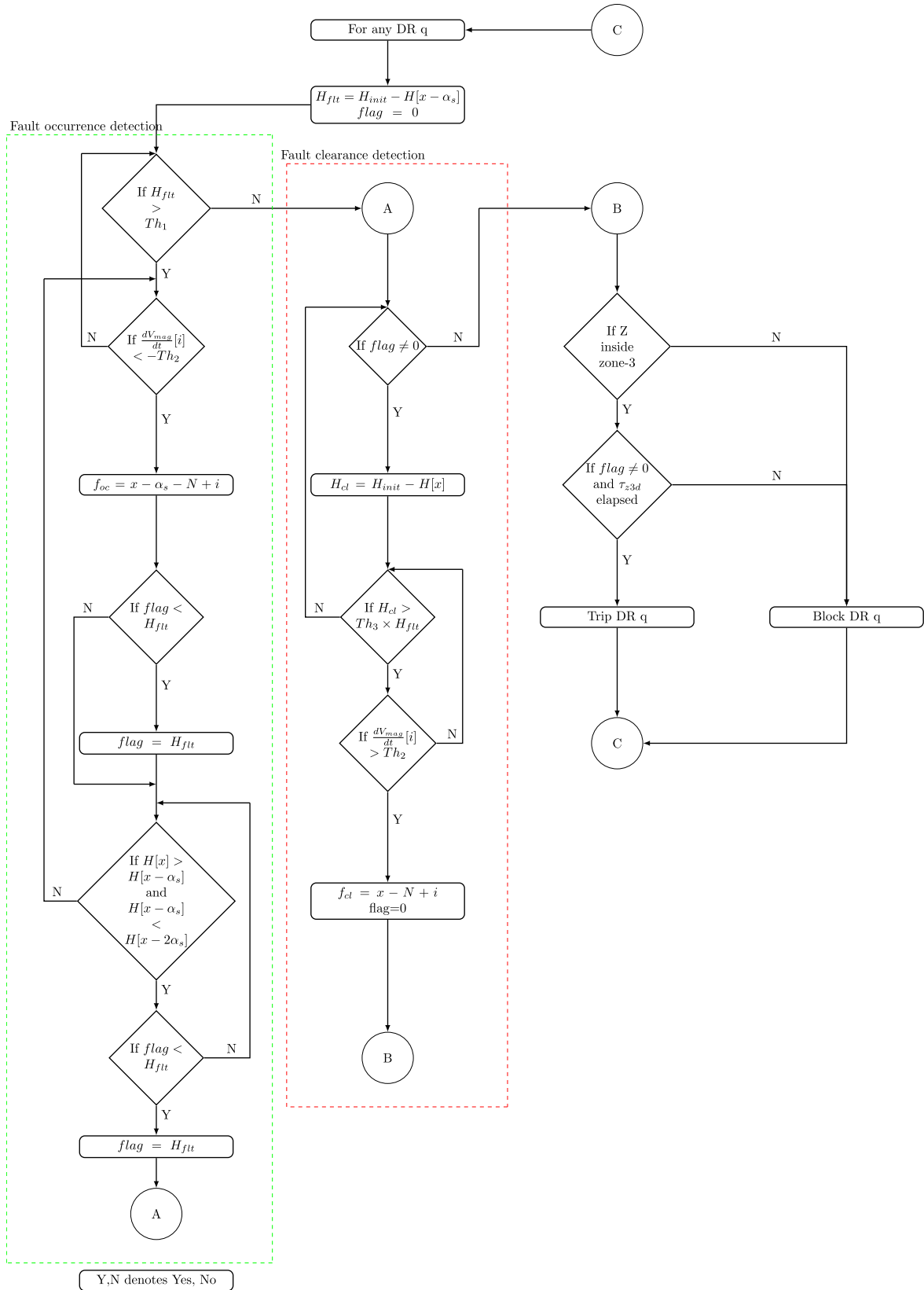
FIGURE 8. Flowchart of the proposed algorithm.

TABLE 1. Case studies.

| Case No	Description
Case study 1	delayed voltage recovery event simulated by delayed clearing of bolted fault with large percentage of induction machine loads
Case study 2	power swing event simulated by tripping of one of the lines connected to the generator
Case study 3	delayed voltage recovery event simulated exclusively by means of ZIP loads
Case study 4	generator outage event at bus 38 to observe the behaviour of distribution entropy for voltage and current signals
Case study 5	line between 21-22 is taken out as contingency to observe the behaviour of distribution entropy for voltage and current signals
Case study 6	delayed voltage recovery event simulated by delayed clearing of resistive fault with large percentage of induction machine loads
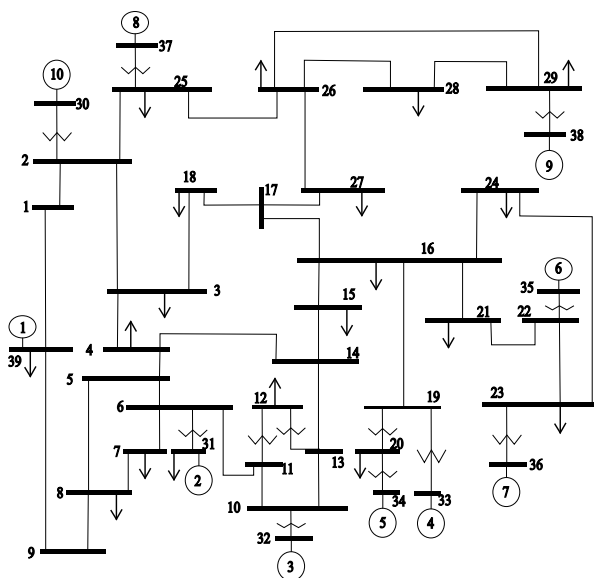
FIGURE 9. 39 bus test system.

IV. SIMULATION RESULTS

A. CASE STUDIES

The proposed algorithm is checked by simulating different case studies as listed in Table.1 for IEEE 39 bus system as it is a representation of the existing New England system [29]. The single line diagram of the test system is displayed in Fig.9. Transient two axis model is considered for all the generators and IEEE Type 1 exciters are modelled at all the generators except the equivalent generator at bus 39. Since delayed voltage recovery events, power swing events are of main concern, which denotes low frequencies are only involved in the events of interest and hence PI model transmission line is chosen. Data for the test system are taken from [19]. A transient stability program is implemented in python and the same is used for simulating case studies. Sampling frequency f_{samp} is considered as 2.5kHz for the 60 Hz test system.
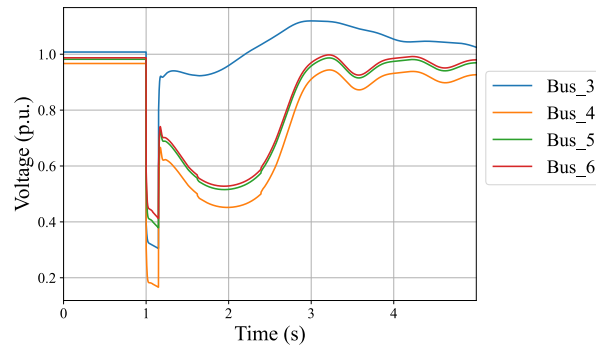

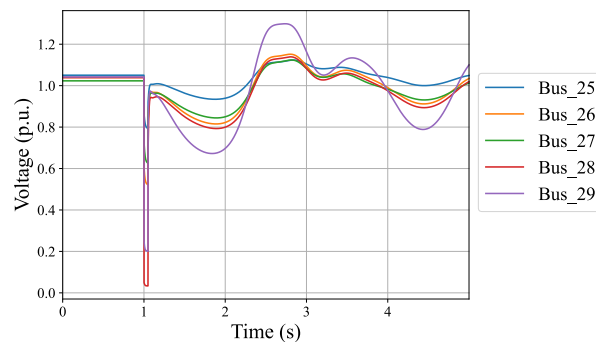**FIGURE 10.** Voltage responses for delayed voltage recovery event.

FIGURE 11. Voltage responses for power swing event.

1) CASE STUDY 1

Load composition at load buses is considered as 70% ZIP load and 30% induction machine loads from the base load scenario [19]. Load composition at Bus 4 is considered as motor load of 402 MVA, 0.866 pf and ZIP load of 160 MW and 80 MVAr. The induction motor parameters are taken from [20] and [30] with the parameters on aggregated machine rating base. Line 4-14 is out of service. A solid three phase fault is created at 50% of the line 3-4 at instant t=1 s and it is cleared by opening the line at t=1.150 s.

The bus voltage responses are shown in Fig.10. It is observed from the plot that the voltages at buses closer to bus 4 are experiencing delayed voltage recovery.

2) CASE STUDY 2

Load composition at all load buses are considered as 70% ZIP load and 30% induction machine loads. A solid three phase fault is created at 20% of the from end of the line 28-29 at t=1 s and it is cleared by opening the line at t=1.050 s. The bus voltage responses are shown in Fig.11. It is observed from the plot that the voltages are oscillating because of a power swing event.

3) CASE STUDY 3

This is a delayed voltage recovery event, indicating momentary recovery in voltage above 0.8 p.u. followed by voltage sag and then voltage recovers back to nominal value. Line 10-11 is out of service. 100% ZIP model is considered
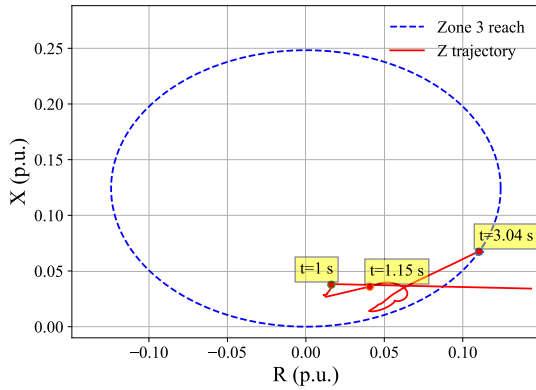
FIGURE 12. R-X plot for DR placed at from end of line 6-5.

FIGURE 13. R-X plot for DR placed at from end of line 5-4.

for all the loads. A solid three phase fault in the middle of the line 16-17 at t=1 s is cleared after 80 ms by opening the line. This is the same case as the first case from [12].

4) CASE STUDY 4
Apart from the equivalent generator at bus 39, the maximum loaded generator is the one located at bus 38 for the base case load scenario considered. Hence the disturbance is created by tripping that generator at t=0.2 s.

5) CASE STUDY 5
Line outage event is simulated by the similar scenario. The heavily loaded line for the base case scenario 22-21 is tripped at t=0.2 s.

6) CASE STUDY 6
Load composition and line data are exactly considered as same as in case 1. A three phase fault with fault resistance of 10 Ω is created at 50% of the line 3-4 at instant t=1 s and it is cleared by opening the line at t=1.16 s. A successive fault is created in bus 4 at t=3 s to check the effectiveness of the proposed algorithm for successive faults following delayed voltage recovery event. The successive fault is cleared at t=3.05 s. Fault resistance has been considered as 10 Ω as the values lies predominantly lesser than that range [31].

B. PERFORMANCE OF THE PROPOSED ALGORITHM
The performance of the proposed algorithm is monitored in the simulated case studies. The distance relay is considered to be mho type and the zone-3 settings are calculated based on [32].

1) CASE STUDY 1
It is shown in Fig.12 that the impedance trajectory enters the zone-3 of the distance relay placed at from end of line 6-5 at the instant of the fault at 1 s and the trajectory lies inside the zone-3 reach even after the fault clearance at 1.15 s uptill 3.04 s.

The impedance trajectory observed by distance relay placed at from end of line 5-4 enters the zone-3 reach at 1 s and leaves at 2.8376 s. It is shown in Fig.13 respectively.
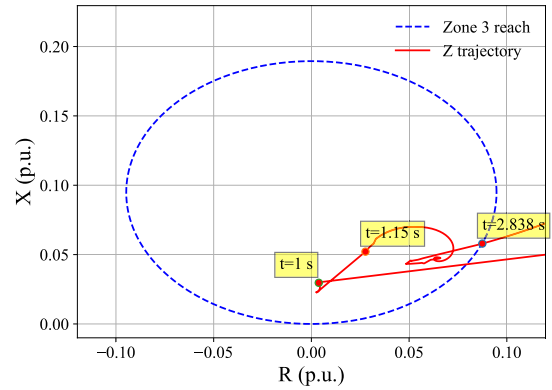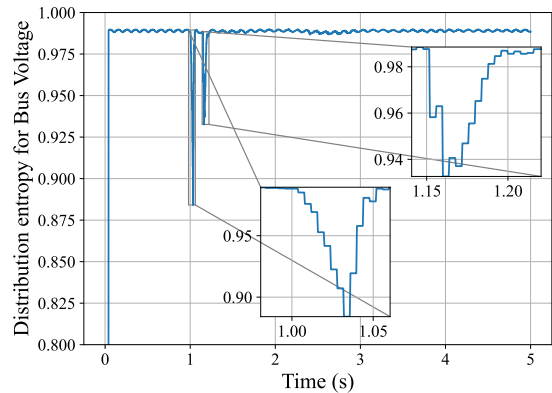

FIGURE 14. Distribution entropy for Bus 6 voltage response.

So even after the fault clearance event, there is a possibility for the impedance trajectory to lie inside the zone-3 of the distance relays. Therefore precise identification of fault occurrence and clearance event is required as mentioned in Section II.

The distribution entropy behaviour monitored by the distance relays placed at the from end of lines 6-5 and 5-4 are shown in Fig.14 and Fig.15 respectively. It is observed that the distribution entropy falls only during fault occurrence and fault clearance events. It is completely stable during voltage recovery. Hence the maloperation of distance relay can be avoided by taking this distribution entropy as an index.

From the Fig.16 and Fig.17, it is evident that the flag for both the relays becomes non zero after the fault occurrence event and goes back to zero after the clearance event is detected by the algorithm.

2) CASE STUDY 2
It is observed from Fig.18 that the impedance trajectory enters the zone-3 of distance relay placed at the from end of line 26-29 at the instant of the fault at 1s and leaves it after fault clearance at 1.05 s. The trajectory enters zone-3 once again at 1.648s and leaves at 2.0704 s.

The distribution entropy for the voltage response at bus 26 is represented for fault occurrence and clearance
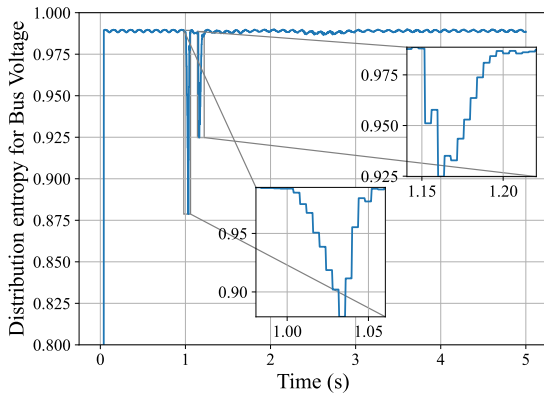
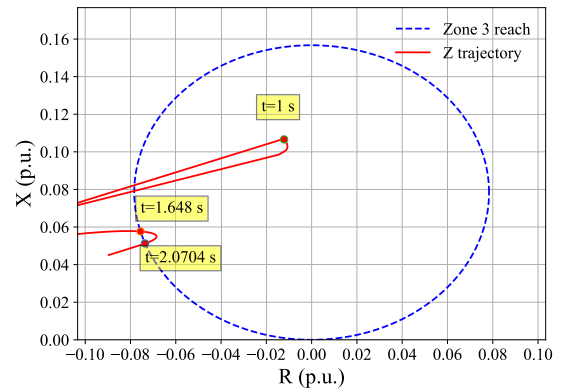**FIGURE 15.** Distribution entropy for Bus 5 voltage response.

FIGURE 16. Distribution entropy flag for DR 6-5.

FIGURE 17. Distribution entropy flag for DR 5-4.

FIGURE 18. R-X plot for DR placed at from end of line 26-29.
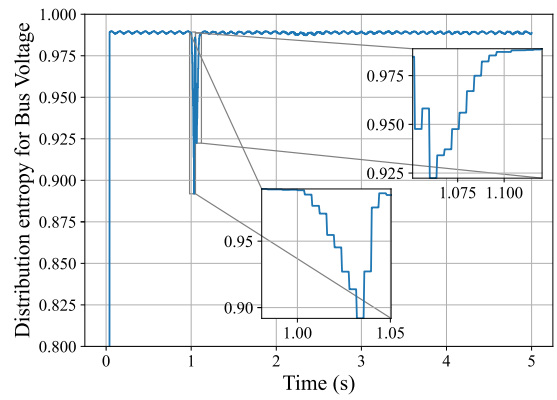

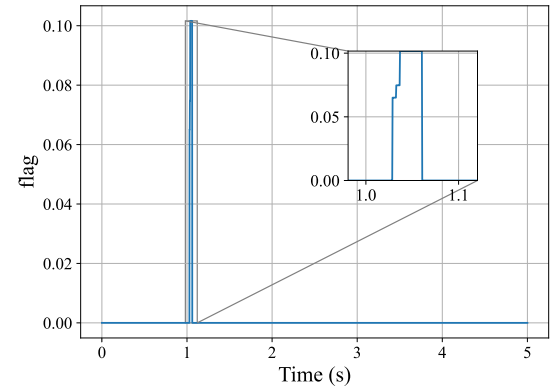**FIGURE 19.** Distribution entropy for Bus 26 voltage response.

FIGURE 20. Distribution entropy flag for DR 26-29.

events in Fig.19. The flag for the distance relay 26-29 is shown in Fig.20.

3) CASE STUDY 3

It is observed from the R-X plot of distance relay 4-14 in Fig.21 that the impedance trajectory enters the zone-3 at 2.1188 s and leaves at 2.4144s.

It is observed from the Fig.22 that the distribution entropy for the bus 4 voltage falls only during fault occurrence and clearance events and the distribution entropy flag for the

distance relay goes back to zero as shown in Fig.23 as the fault clears.

4) CASE STUDY 4

It is observed from the Fig.24 that distribution entropy value for bus voltage does not change significantly whereas from Fig.25, the distribution entropy value changes significantly for line current.

5) CASE STUDY 5

It is observed from Fig.26 and Fig.27 that distribution entropy value for bus voltage does not change significantly for line
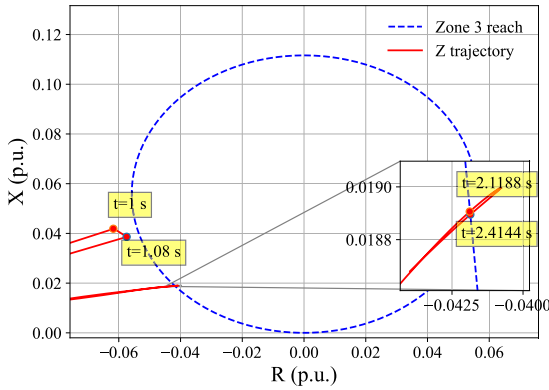
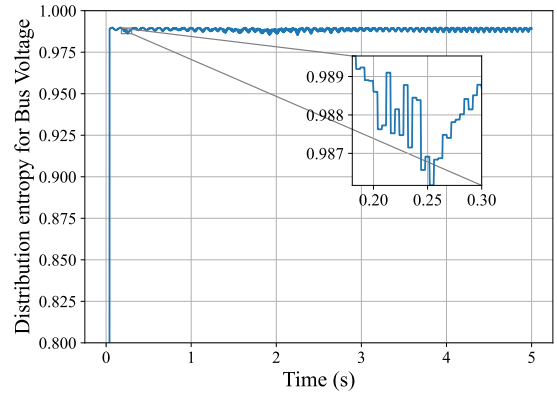**FIGURE 21.** R-X plot for DR placed at from end of line 4-14.

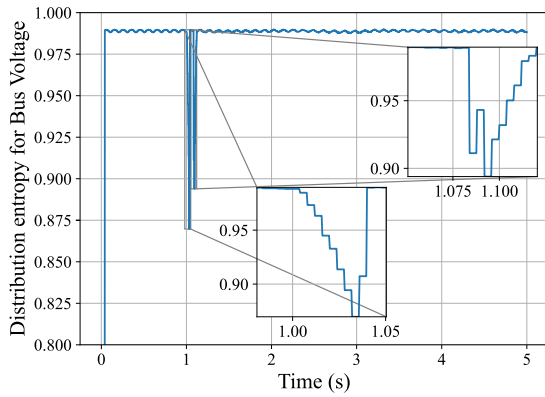**FIGURE 22.** Distribution entropy for Bus 4 voltage response.

FIGURE 23. Distribution entropy flag for DR 4-14.

FIGURE 24. Distribution entropy for Bus 29 voltage response.

FIGURE 25. Distribution entropy for line current of DR 29-28.
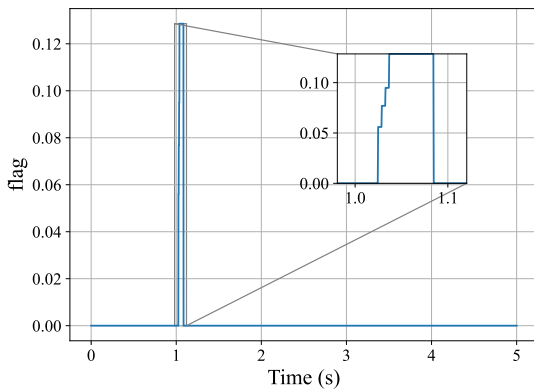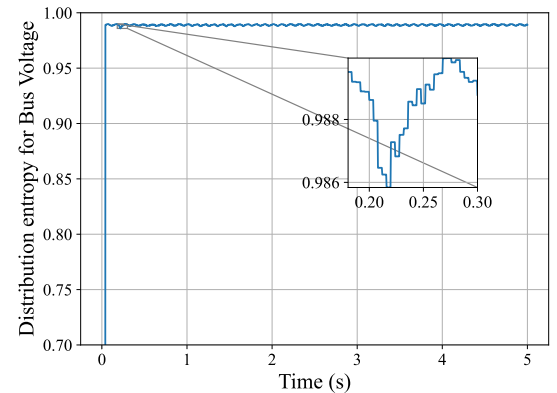

FIGURE 26. Distribution entropy for Bus 22 voltage response.

outage event at DRs placed on line 21-22 and 22-21. From Fig.28 and Fig.29, it is evident that the distribution entropy value for line current changes significantly for both the relays.

6) CASE STUDY 6

From Fig.30 and Fig.31, it is observed that the impedance trajectory seen by the DRs placed at from end of lines 6-5, and 5-4 enters zone-3 reach at time t=1 s and stays inside the zone-3 reach even after the fault clearance at t=1.16 s up till t=2.05 s and t=1.84 s respectively. Similarly, for

the successive fault at t=3 s, from Fig.32 and Fig.33, the impedance trajectories enters the zone-3 reach of the relays again and leaves after the fault gets cleared.

As observed from Fig.34 and Fig.35, the flag for distance relays at from end of lines 6-5, 5-4 goes non-zero only during faults.

C. COMPARISON WITH RECENT LITERATURE

Even though the local signal based methods in the literature have considered identifying the fault clearance events for the
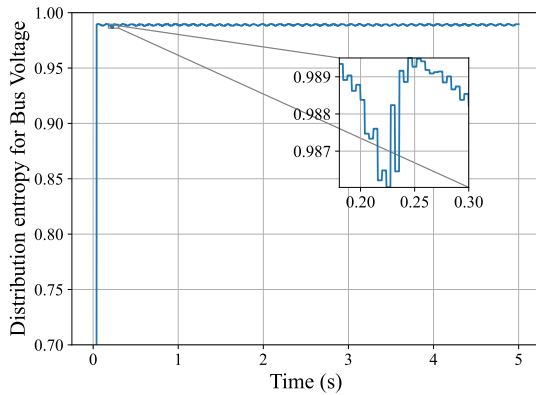
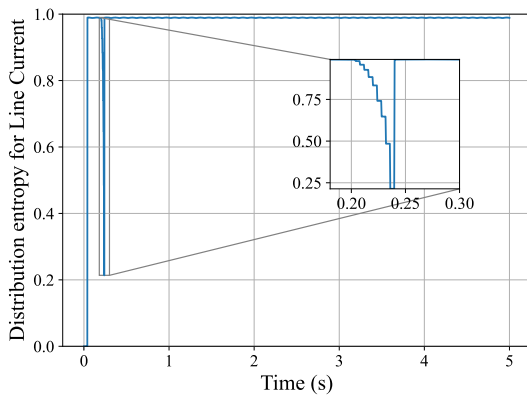**FIGURE 27.** Distribution entropy for Bus 21 voltage response.

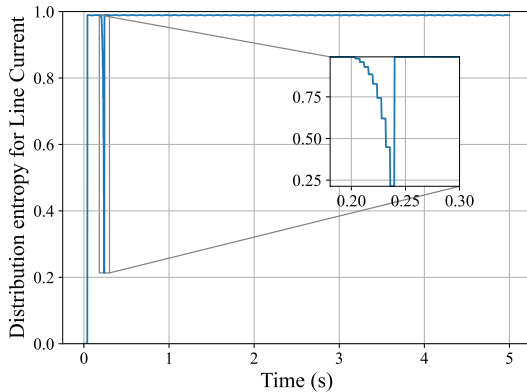**FIGURE 28.** Distribution entropy for line current of DR 22-21.

FIGURE 29. Distribution entropy for line current of DR 21-22.

FIGURE 30. R-X plot for DR placed on from end of line 6-5 at t=1 s.
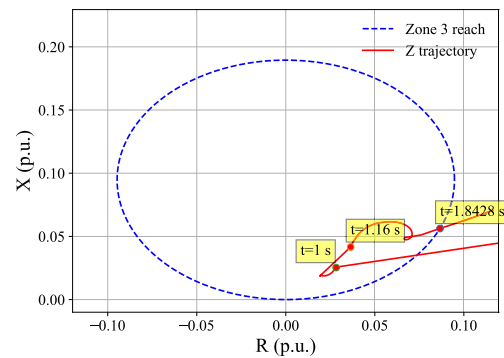
FIGURE 31. R-X plot for DR placed on from end of line 5-4 at t=1 s.
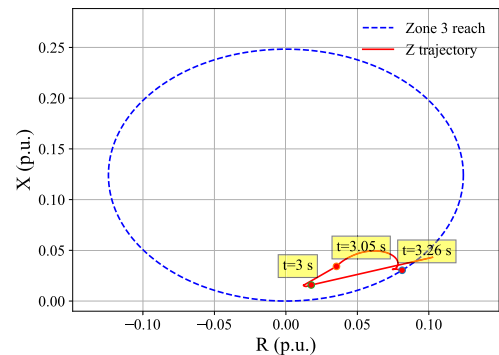
FIGURE 32. R-X plot for DR placed on from end of line 6-5 at t=3 s.

necessity of identifying maloperating zone-3 distance relays, they have used higher sampling frequency [15].

In [12], the method basically identifies if the impedance trajectory is closing onto the zone-3 of the distance relay and then blocks the relay from operation based on the zone-3 blocking index calculated. However if the impedance trajectory lies inside the zone-3 even after the fault clearance as shown in case study 1, then the existing method is no longer applicable for such a scenario. The proposed method in turn identifies the fault occurrence and fault clearance events and
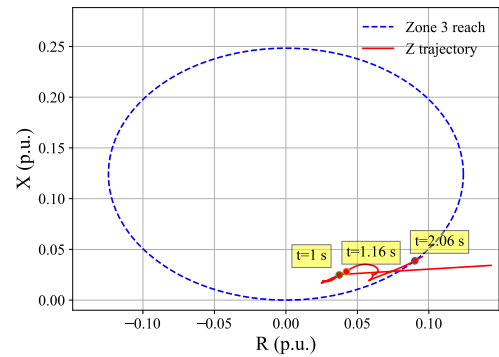
blocks the zone-3 of the relay from operation for non fault events.

Hence from the Table.2, it is observed that the desired operation of the relay is met by the proposed method and the method adopted in [12] is not applicable under certain circumstances.

D. TIME TAKEN FOR THE PROPOSED ALGORITHM

The time taken for the proposed algorithm is validated with a host computer with the hardware configuration of Intel Core i7 processor - 7700 (CPU), 3.6 GHz and 16 GB RAM. The time taken for computation of distribution entropy value and approximate entropy value is around 1.2 ms and 2.1 ms respectively.

FIGURE 33. R-X plot for DR placed on from end of line 5-4 at t=3 s.

FIGURE 34. Distribution entropy flag for DR 6-5.

FIGURE 35. Distribution entropy flag for DR 5-4.

The operations required for calculating distribution entropy for an instantaneous signal of moving window length N and embedding dimension m is $(N 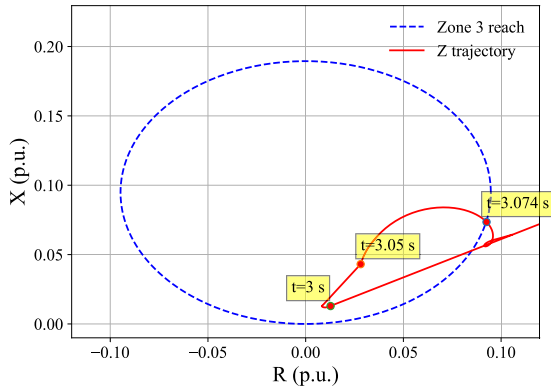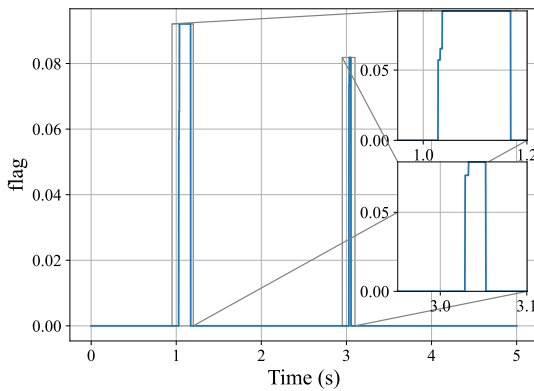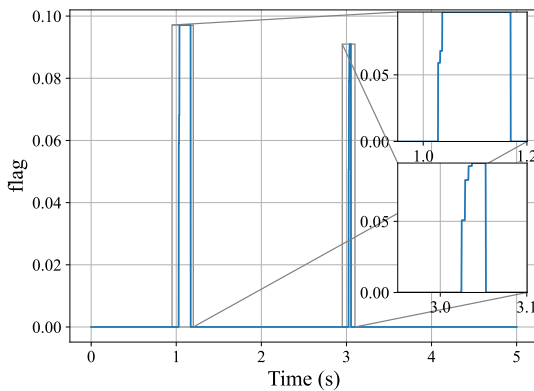- m) \times (N - m + 1) = N^2 - 2mN + N + m^2 - m$ [17] and for approximate entropy is $2N^2 + N(6 - 4m) + 2m^2 - 6m + 7$ [33]. Considering N as 100 and m as 2, the total number of operations required for calculating approximate entropy, sample entropy, distribution entropy are 19803, 19405, and 9702 respectively. From [34], the execution time for the sample entropy of a sine data in FPGA has been evaluated

TABLE 2. Expected relay operation.

Case No and Relay	Time duration	Proposed method	Method in [12]	Desired Operation
Case study 1, 6-5	1.15-3.04 s	Block	Not applicable	Block
Case study 1, 5-4	1.15-2.838 s	Block	Not applicable	Block
Case study 2, 26-29	1.648-2.071 s	Block	Block	Block
Case study 3, 4-14	2.118-2.414 s	Block	Block	Block
Case study 6, 6-5	1.15-2.05 s	Block	Not applicable	Block
Case study 6, 5-4	1.16-1.84 s	Block	Not applicable	Block

TABLE 3. Security index and dependability index with and without the proposed algorithm.

Number of operations	Zone-3 operation with proposed algorithm	Zone-3 operation without proposed algorithm
No. of correct zone-3 operations	8	8
No. of unwanted zone-3 operations	0	2
No. of failures to operate zone-3	0	0
Security index(%)	100	80
Dependability index(%)	100	100

to be around 2 ms for a data length of 100 samples. Therefore the proposed distribution entropy based method can operate much faster in real time compared to other methods in real time. There is a substantial decrease in the number of operations for calculating distribution entropy compared to combined computational cost of approximate entropy and wavelet. The time taken for the proposed algorithm to identify a fault occurrence and fault clearance event is 2 cycles and 1 cycle respectively.

E. CALCULATION OF SECURITY INDEX AND DEPENDABILITY INDEX FOR THE ZONE-3 DISTANCE RELAY WITH AND WITHOUT THE PROPOSED ALGORITHM

For the calculation of security index and dependability index, a modified 39 bus system with additional different scenarios are considered.

Security index is defined as

$$S = \frac{N_C}{N_C + N_U} \quad (6)$$

where N_C and N_U refers to number of correct zone-3 operations and number of unwanted zone-3 operations respectively.

Dependability index is defined as

$$D = \frac{N_C}{N_C + N_F} \quad (7)$$

where N_C and N_F refers to number of correct zone-3 operations and number of failures to operate zone-3 respectively.

For the limited number of cases considered, the Table.3 results indicate that the percentage of security index is much better for the operation of distance relay with proposed algorithm compared to without the algorithm. There is no change to the percentage of dependability index with and without the proposed algorithm.

V. CONCLUSION

A distribution entropy based algorithm is proposed in this paper which identifies the fault occurrence and clearance events clearly with a lesser time. This is used to block the zone-3 distance relays from operation for non fault events even if the trajectory lies inside the zone-3 reach after the fault clearance. The algorithm has been validated with 39 bus test system for different cases. The zone-3 distance relay operation with the proposed algorithm is compared with the desired operation of the relay for different cases. The heavily loaded generator and lines are tripped for checking the stability of the proposed algorithm for contingency cases.

Compared with the existing literature, it can be inferred from the results that the proposed method was able to prevent the relays from maloperation for non-fault events and operates it only for fault events. However, the method may not be suitable for distance relays to identify high resistance faults. The suggested approach functions well for most scenarios since resistive faults occurring in transmission system is of the order of 10Ω or lesser. The selection of threshold requires extensive simulations to be run under different contingencies. In-spite of the minor limitations, the distance relay operation with the proposed algorithm enhances the security index by 20% without endangering the dependability index.

REFERENCES

[1] H. Ferrer, E. Schweitzer, and S. E. Laboratories, *Modern Solutions for Protection, Control, and Monitoring of Electric Power Systems*. Pullman, WA, USA: Schweitzer Engineering Laboratories, 2010.

[2] K. Seethalekshmi, S. N. Singh, and S. C. Srivastava, "A classification approach using support vector machines to prevent distance relay maloperation under power swing and voltage instability," *IEEE Trans. Power Del.*, vol. 27, no. 3, pp. 1124–1133, Jul. 2012, doi: 10.1109/TPWRD.2011.2174808.

[3] M. Arumuga and M. J. B. Reddy, "Distance protection methodology for detection of faulted phase and fault along with power swing using apparent impedance," *IEEE Access*, vol. 10, pp. 43583–43597, 2022, doi: 10.1109/ACCESS.2022.3168563.

[4] P. K. Nayak, A. K. Pradhan, and P. Bajpai, "Secured zone 3 protection during stressed condition," *IEEE Trans. Power Del.*, vol. 30, no. 1, pp. 89–96, Feb. 2015, doi: 10.1109/TPWRD.2014.2348992.

[5] D. Kang and R. Gokaraju, "A new method for blocking third-zone distance relays during stable power swings," *IEEE Trans. Power Del.*, vol. 31, no. 4, pp. 1836–1843, Aug. 2016, doi: 10.1109/TPWRD.2016.2520394.

[6] M. S. Parniani, M. Sanaye-Pasand, and P. Jafarian, "A blocking scheme for enhancement of distance relay security under stressed system conditions," *Int. J. Electr. Power Energy Syst.*, vol. 94, pp. 104–115, Jan. 2018, doi: 10.1016/j.ijepes.2017.06.020.

[7] T. Jose, M. Biswal, K. Venkatanagaraju, and O. P. Malik, "Integrated approach based third zone protection during stressed system conditions," *Electric Power Syst. Res.*, vol. 161, pp. 199–211, Aug. 2018, doi: 10.1016/j.epsr.2018.04.011.

[8] K. Venkatanagaraju, M. Biswal, and R. C. Bansal, "Adaptive distance relay algorithm to detect and discriminate third zone faults from system stressed conditions," *Int. J. Electr. Power Energy Syst.*, vol. 125, Feb. 2021, Art. no. 106497, doi: 10.1016/j.ijepes.2020.106497.

[9] B. Sahoo, S. R. Samantaray, and B. R. Bhalja, "An effective zone-3 supervision of distance relay for enhancing wide area back-up protection of transmission system," *IEEE Trans. Power Del.*, vol. 36, no. 5, pp. 3204–3213, Oct. 2021, doi: 10.1109/TPWRD.2020.3035885.

[10] V. Nougain, M. K. Jena, and B. K. Panigrahi, "Synchro-phasors assisted back-up protection of transmission line," *IET Gener., Transmiss. Distrib.*, vol. 12, no. 14, pp. 3414–3420, May 2018, doi: 10.1049/iet-gtd.2017.1711.

[11] B. Sahoo, S. R. Samantaray, and I. Kamwa, "Supervising vulnerable third zone distance relay to enhance wide-area back-up protection systems," *IEEE Access*, vol. 10, pp. 49862–49872, 2022, doi: 10.1109/ACCESS.2022.3173755.

[12] J. D. Ashkezari, M. E. H. Golshan, and A. Mirzaei, "Secured zone 3 operation against fault induced delayed voltage recovery event," *IEEE Trans. Power Del.*, vol. 37, no. 1, pp. 507–516, Feb. 2022, doi: 10.1109/TPWRD.2021.3063923.

[13] Y. Zhang, Y. Xu, Z. Y. Dong, and P. Zhang, "Real-time assessment of fault-induced delayed voltage recovery: A probabilistic self-adaptive data-driven method," *IEEE Trans. Smart Grid*, vol. 10, no. 3, pp. 2485–2494, May 2019, doi: 10.1109/TSG.2018.2800711.

[14] V. C. Nikolaidis, "Emergency zone 3 modification as a local response-driven protection measure against system collapse," *IEEE Trans. Power Del.*, vol. 31, no. 5, pp. 2114–2122, Oct. 2016, doi: 10.1109/TPWRD.2016.2552644.

[15] A. M. Abdullah, "A new solution for improving transmission line distance protection security during system-wide cascading failures," Ph.D. thesis, Dept. Elec. Eng., Texas A & M Uni., College Station, TX, USA, May 2018. [Online]. Available: https://oaktrust.library.tamu.edu/handle/1969.1/173579

[16] L. Fu, Z. Y. He, R. K. Mai, and Z. Q. Bo, "Approximate entropy and its application to fault detection and identification in power swing," in *Proc. IEEE Power Energy Soc. Gen. Meeting*, Calgary, AB, Canada, Jul. 2009, pp. 1–8, doi: 10.1109/PES.2009.5275380.

[17] R. Udhayakumar, C. Karmakar, P. Li, X. Wang, and M. Palaniswami, "Modified distribution entropy as a complexity measure of heart rate variability (HRV) signal," *Entropy*, vol. 22, no. 10, p. 1077, Sep. 2020, doi: 10.3390/e22101077.

[18] V. Vittal, J. McCalley, P. Anderson, and A. Fouad, *Power System Control and Stability* (IEEE Press Series on Power and Energy Systems). 3rd ed., Hoboken, NJ, USA: Wiley, 2019. [Online]. Available: https://books.google.co.in/books?id=obCuDwAAQBAJ

[19] M. Pai, *Energy Function Analysis for Power System Stability* (Power Electronics and Power Systems). Berlin, Germany: Springer, 2012.

[20] W. W. Price, C. W. Taylor, and G. J. Rogers, "Standard load models for power flow and dynamic performance simulation," *IEEE Trans. Power Syst.*, vol. 10, no. 3, pp. 1302–1313, Aug. 1995, doi: 10.1109/59.466523.

[21] J. D. Ashkezari and M. E. H. Golshan, "A monitoring and modifying scheme for zone 3 of critical distance relays in view of voltage stability," *Electric Power Syst. Res.*, vol. 183, Jun. 2020, Art. no. 106273, doi: 10.1016/j.epsr.2020.106273.

[22] (Jun. 2019). *Transmission System Planning Performance*. Western Electricity Coordinating Council. [Online]. Available: https://www.wecc.org/Reliability/TPL-001-WECC-CRT-3.2.pdf

[23] (Jun. 2022). *Whitepaper on Transient Voltage Response Criteria*. North American Electricity Reliability Corporation. [Online]. Available: https://www.nerc.com/comm/RSTC_Reliability_Guidelines/Whitepaper_on_Transient_Voltage_Response_Criteria_12_06_2022.pdf

[24] P. Li, C. Liu, K. Li, D. Zheng, C. Liu, and Y. Hou, "Assessing the complexity of short-term heartbeat interval series by distribution entropy," *Med. Biol. Eng. Comput.*, vol. 53, no. 1, pp. 77–87, Jan. 2015, doi: 10.1007/s11517-014-1216-0.

[25] R. J. Hyndman. (1995). *The Problem With Sturges' Rule for Constructing Histograms*. [Online]. Available: https://robjhyndman.com/papers/sturges.pdf

[26] R. K. Udhayakumar, C. Karmakar, P. Li, and M. Palaniswami, "Effect of embedding dimension on complexity measures in identifying arrhythmia," in *Proc. 38th Annu. Int. Conf. IEEE Eng. Med. Biol. Soc. (EMBC)*, Aug. 2016, pp. 6230–6233, doi: 10.1109/EMBC.2016.7592152.

[27] M. W. Flood and B. Grimm, "EntropyHub: An open-source toolkit for entropic time series analysis," *PLoS ONE*, vol. 16, no. 11, Nov. 2021, Art. no. e0259448, doi: 10.1371/journal.pone.0259448.

[28] D. Sun, H. Zhang, and Z. Guo, "Complexity analysis of precipitation and runoff series based on approximate entropy and extreme-point symmetric mode decomposition," *Water*, vol. 10, no. 10, p. 1388, Oct. 2018, doi: 10.3390/w10101388.

[29] T. Athay, R. Podmore, and S. Virmani, "A practical method for the direct analysis of transient stability," *IEEE Trans. Power App. Syst.*, vol. PAS-98, no. 2, pp. 573–584, Mar. 1979, doi: 10.1109/TPAS.1979.319407.

[30] B. Seshaprasad and D. Mikkelsen, "Load models for power system stability studies," in *Proc. Nat. Power Syst. Conf.*, 2000, pp. 166–171.

[31] A. dos Santos, C. Gaspar, M. T. C. de Barros, and P. Duarte, "Transmission line fault resistance values based on field data," *IEEE Trans. Power Del.*, vol. 35, no. 3, pp. 1321–1329, Jun. 2020, doi: 10.1109/TPWRD.2019.2941432.

[32] M. Chen, H. Wang, S. Shen, and B. He, "Research on a distance relay-based wide-area backup protection algorithm for transmission lines," *IEEE Trans. Power Del.*, vol. 32, no. 1, pp. 97–105, Feb. 2017, doi: 10.1109/TPWRD.2016.2599198.

[33] J. Tomč ala, "New fast ApEn and SampEn entropy algorithms implementation and their application to supercomputer power consumption," *Entropy*, vol. 22, no. 8, p. 863, Aug. 2020, doi: 10.3390/e22080863.

[34] C. Chen, B. da Silva, R. Chen, S. Li, J. Li, and C. Liu, "Evaluation of fast sample entropy algorithms on FPGAs: From performance to energy efficiency," *Entropy*, vol. 24, no. 9, p. 1177, Aug. 2022. [Online]. Available: https://www.mdpi.com/1099-4300/24/9/1177

UPENDRAN MUKUNDARAJAN received the B.E. degree in electrical and electronics engineering from the Sona College of Technology, Salem, in 2012, and the M.Tech. degree in electrical engineering from Indian Institute of Technology, Banaras Hindu University, Varanasi, in 2017. He is currently pursuing the Ph.D. degree with the Department of Electrical Engineering, Indian Institute of Technology Madras.

From 2017 to 2019, he was a Research and Development Engineer with the Power Research and Development Consultants Pvt. Ltd., Bengaluru. His research interests include delayed voltage recovery events and distance protection.

K. SHANTI SWARUP (Senior Member, IEEE) is currently with the Department of Electrical Engineering, Indian Institute of Technology Madras, Chennai, India. Prior to joining the department, he held positions with Mitsubishi Electric Corporation, Osaka, Japan, and Kitami Institute of Technology, Hokkaido, Japan, as a Research Scientist and a Visiting Professor, from 1992 to 1999. Since 2000, he has been a regular faculty. His research interests include power systems computer modeling, simulation, energy management systems, deregulation, automation, numerical/digital protection, and smart power grids.

• • •